Investigation of special features of parameters of Schottky barrier contacts caused by a nonlinear bias dependence of the barrier height

V. G. Bozhkov and A. V. Shmargunov[a)]
CJSC "Scientific Research Institute of Semiconductor Devices" 634034, Tomsk, Russia

(Received 25 November 2011; accepted 3 February 2012; published online 8 March 2012)

The results of studying the IV-characteristics (IVCs) of the contact Au-n-GaAs obtained by electrochemical deposition are presented. The observed characteristics - the bias dependence of the ideality factor (n), the measured (φ_{bm}) and effective (φ_{bI}) barrier heights, an inverse relationship between the measured barrier height and ideality factor, and the edge effects (the dependence of n, φ_{bm}, and φ_{bI} on the contact diameter) are explained by the nonlinear bias dependence on the effective barrier height. The explanation is given on the basis of the contact model with an intermediate layer and interface states (Bardeen model), and the intimate contact model with the subsurface states. The nonlinearity of the bias dependence on the barrier height is due to the inhomogeneous energy distribution of the interface states (a decrease in density from the edges to the middle of the bandgap) and the inhomogeneous energy and coordinate (from the surface to the depth) distribution of the subsurface states. An essential feature for every model is also the condition that the barrier height and ideality factor are measured at a constant current (or in a constant range of currents) while studying contacts with different diameters or when measuring the IVCs at different temperatures. This condition is not difficult to achieve, but gives the necessary certainty to different barrier height values used in examining experimental results. Some limitations and shortcomings of the widely used model of inhomogeneous Schottky barrier contact with the "saddle points" are also discussed. © *2012 American Institute of Physics*. [http://dx.doi.org/10.1063/1.3691959]

I. INTRODUCTION

It is well known that despite rather extensive and lengthy investigations, the reasons for fairly numerous "anomalies" (or special features) in the behavior of the measured characteristics of the Schottky barrier contacts (SBC) remain controversial. The most-studied "anomaly" of this kind is an increase of the ideality factor n of the current-voltage characteristics (IVCs) of contacts, and a simultaneous decrease in the barrier height φ_{bm} measured by the saturation current with decreasing temperature. Other features of real Schottky barrier contacts may include the well-known difference between the barrier heights determined from the I-V- and C-V-characteristics (φ_b and φ_{bc}, respectively),[1] the presence of peripheral (edge) effects in the contacts,[2–7] as well as the inverse relationship between the barrier height and ideality factor found from IVCs,[8–11] which is widely used to determine the barrier height of the homogeneous contact.[9,12]

Among researchers, the most widespread hypothesis assumes lateral inhomogeneity of the barrier height in the contacts as a cause of almost all the observed anomalies in their characteristics. According to Ref. 13 the low-temperature behavior of the IVCs and the difference in the barrier heights φ_b and φ_{bc} can be explained by the Gaussian distribution of the barrier height over the area of the contact, whose parameters (the standard deviation and average barrier height) depend on the bias. According to the authors of Refs. 14 and 15 the determining factor is the inhomogeneity of the contact in the form of the so-called "saddle points" arising in the contact under specific conditions, when a small area of a contact with low barrier height is surrounded by a region with great barrier height (as a result of "pinch-off effect").

The existence of inhomogeneity in the contact barrier height is not in doubt. It is confirmed by direct studies of the distribution of the barrier height in contacts with ballistic electron emission microscopy (a BEEM-method).[16] However, studies[17–24] (and others) evidently do not indicate that the "saddle points" play the main role in the observed "anomalies" in the contact characteristics, but do not exclude other factors playing a similar role. It should also be noted that for comparison with experiment, a highly simplified version of the model of "saddle points" with the IVC significantly different from the exact expression[25] (Eq. (5.3.8)) is used. As for the assumption regarding linear decrease in dispersion of the barrier height with increasing bias, which is required to explain the "low-temperature anomaly" of IVC according to Ref. 13 it has no physical grounds to date.

We believe that attempts to explain "anomalies" in the Schottky barrier characteristics on the basis of only nonuniform distribution of the barrier height of a certain type are groundless. The most acceptable basis for such an explanation is, in our opinion, the consideration of the effect of the nonlinear bias dependence of the barrier height (hereinafter, the nonlinearity of the barrier height) on the parameters of the contacts n and φ_{bm}, combined with the assumption that these parameters are measured at a specified (constant) current for different temperatures and (or) diameters.[26,27]

a)Author to whom correspondence should be addressed. Electronic mail: tohsh@list.ru.

The latter seems to be quite natural in studying the dependences of the IVC on the temperature or contact diameter.

As it turned out, even taking into account the nonlinearity of the barrier height caused only by the image-force effect results in a "low-temperature anomaly" of IVC shifted to lower temperatures.[28] Nonlinearity of the barrier height with the same result (a manifestation of the "low-temperature anomaly") can be caused by an increase in the density of the interface states (ISs) to the edges of the semiconductor bandgap[29–31] and by a similar increase in the density of subsurface states (SSS) and their distribution over the coordinate in intimate contacts.[32] The nonlinear behavior of the effective barrier height is also typical of contact with the Gaussian distribution of the barrier height, if the effect of the series resistance of local areas of contact on the IVC is taken into account.[33,34] For a model of an inhomogeneous contact presented in Refs. 14 and 15 and for a tunnel contact,[35,36] the nonlinearity of the barrier height is though not unique, but an important reason for "anomalies" in their characteristics. Therefore, it should be taken into account in the analysis of IVCs.

The purpose of this paper is to show experimentally, by example, the Au-n-GaAs contacts, that taking into account the nonlinear bias dependence of the barrier height caused by the non-uniform distribution of ISs and SSSs, makes it possible to explain not only the low-temperature,[30,31] but also other "anomalies " of SBCs: The edge effects in the contacts and inverse relationship between the measured barrier height and ideality factor of IVC, which was previously attributed only to the inhomogeneity of the barrier height.[9–12] The first of these "anomalies" is due to the characteristic distribution of the state density over the energy and coordinate. The second, as shown, may be due to fluctuations of the IS or SSS parameters.

II. BASIC THEORETICAL POSITIONS

To compare the experiment and calculation, we consider a well-known model of contacts with a transparent intermediate layer and surface (interface) states (for brevity, the Bardeen model, BM)[31] and a model of an intimate contact (IC) with subsurface states.[32] In both cases, we are talking about inhomogeneously distributed (over energy) states that are in equilibrium (interact) with the semiconductor. There are also states that are in equilibrium with metal and pin the Fermi level. It is known that a classical Bardeen model is characterized by just such states.[37] An attribution of two types of states to this model is an assumption, which however has convincing experimental evidence (see, for example, Ref. 38, and references therein).

A. The Bardeen model

In the Bardeen model (Fig. 1), the barrier height is determined by the relation,

$$\varphi_b(V) = \varphi_b(0) + V_{\delta i}(V) \equiv \varphi_{b0} + V_{\delta i}(V). \tag{1}$$

In accordance with the thermionic-emission theory, IVC can be represented in the form,[1,37]

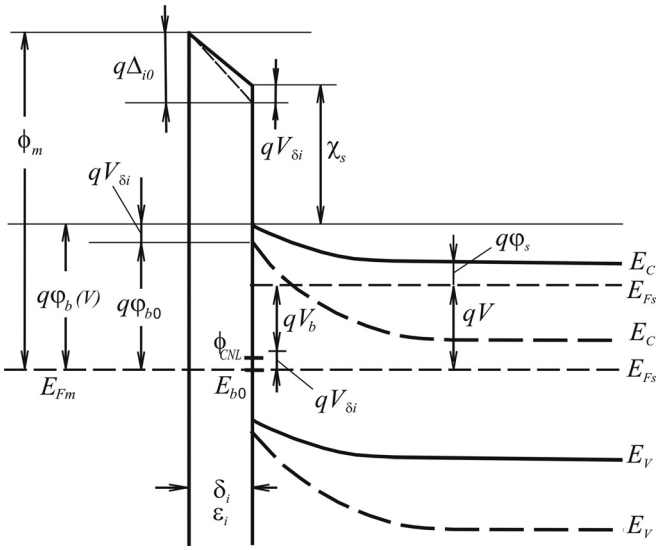

FIG. 1. Energy diagram of the M-S Schottky barrier contact with an intermediate layer and interface states (not shown in the figure) - the Bardeen model. Dashed lines – equilibrium state, solid lines – state with applied bias V; ϕ_m - work function, χ_s - affinity, ϕ_{CNL} - the charge neutrality level, E_{b0} - level, around which the Fermi level is pinned (equilibrium level).

$$I = AR^*T^2\exp\left(-\frac{q\varphi_b(V)}{kT}\right)\exp\left(\frac{q(V-IR_s)}{kT}\right). \tag{2}$$

Here A is the contact area, R^* is the Richardson constant, T is the absolute temperature, q is the electron charge, k is the Boltzmann constant, and R_s is the series contact resistance (some of the designations are shown in Fig. 1). As seen from the figure, the contact bias is distributed between the intermediate layer ($V_{\delta i}$) and the barrier region (V_b),

$$V = V_{\delta i} + V_b. \tag{3}$$

Note that we also consider Eq. (2) as the definition of the real barrier height and, in the general case, as an effective barrier height $\varphi_b(V)$.[31,32]

Usually, it is assumed that the barrier height is a weak linear function of bias,[1] but here, we take into account its nonlinearity. Therefore, the ideality factor of IVC defined as

$$n(V) = \frac{q}{kT}\frac{dV}{d\ln I} = \left[1 - \frac{d\varphi_b(V)}{dV}\right]^{-1} \tag{4}$$

becomes the bias function.[1] The well-known IVC-approximation for determining the ideality factor and barrier height has the following form:

$$I = AR^*T^2\exp\left(-\frac{q\varphi_{bm}(V)}{kT}\right)\exp\left(\frac{q(V-IR_s)}{n(V)kT}\right)$$
$$= I_s\exp\left(\frac{q(V-IR_s)}{n(V)kT}\right). \tag{5}$$

Here $\varphi_{bm}(V)$ and $n(V)$ are the barrier height measured from the saturation current (hereafter, the measured barrier height) and the slope of the IVC in the semi-logarithmic scale, respectively. These parameters characterize the IVC (2) at a certain bias value V, where IVC (5) is a tangent to the IVC

(2) in the semi-logarithmic scale. A comparison of IVCs (2) and (5) (equating them at the point of tangency) allows us to relate an effective barrier height $\varphi_b(V)(\equiv \varphi_{bI})$ to the measured $\varphi_{bm}(V)$ at a given current independent of the contact diameter

$$\varphi_{bm} = \frac{kT}{q}\ln\left(\frac{AR^*T^2}{I_s}\right) \tag{6}$$

using the relation given in[26,27]

$$\varphi_{bI} = n\varphi_{bm} - (n-1)\frac{kT}{q}\ln\frac{AR^*T^2}{I} = \varphi_{bn} - (n-1)\frac{kT}{q}\ln\frac{AR^*T^2}{I}. \tag{7}$$

If necessary, the concept of barrier height at a given bias φ_{bV} can be introduced.[26,27] Here, we introduce also another designation $\varphi_{bn} \equiv n\varphi_{bm}$. This quantity is often used as the barrier height, because of the close match with the real barrier height (see, for example, Refs. 39 and 40).

Note that the expression (7) retains its form also for the case $n = const$ with the difference that in this case, $\varphi_{bm} = \varphi_{b0} = const$. For flat bands, where $I = I_{bf}$ ($I_{bf} = AR^*T^2\exp(-q\varphi_s/kT)$ is the flatband current[41]), this expression, as already mentioned,[26,27] is transformed into a well-known relation for the flat-band barrier height φ_{bf},[42]

$$\varphi_{bf} = n\varphi_{b0} - (n-1)\varphi_s, \tag{8}$$

where $\varphi_{b0} \equiv \varphi_b(V=0)$ and $q\varphi_s = E_C - E_{Fs} = kT\ln(N_C/N_D)$ (see Fig. 1), N_C is the effective state density in the conduction band, and N_D is the concentration of ionized donor impurity in the semiconductor.

Determination of the barrier height φ_b at any bias voltage (the dependence $\varphi_b(V)$) is reduced, according to Eq. (1), to the determination of an equilibrium barrier height φ_{b0} and the portion of the bias $V_{\delta I}$ that drops in the intermediate layer at a given bias. The value of φ_{b0} is calculated from the condition of the charge balance in the contact in equilibrium as follows:

$$Q_m + Q_{sc} + Q_{ss} = 0. \tag{9}$$

It is convenient to define the voltage $V_{\delta i}$ from the condition of the charge balance under bias voltage applied in the following form:

$$\Delta Q_m(V) + \Delta Q_{sc}(V) + \Delta Q_{ss}(V) = 0, \tag{9a}$$

where Q_m, Q_{sc}, and Q_{ss} are the charges in the metal, barrier, and surface (interface) states, respectively,

$$Q_m(V) = -\frac{\varepsilon_i(\Delta_{i0} - V_{\delta i})}{\delta_i} = -C_{\delta i}(\Delta_{i0} - V_{\delta i}) \tag{10}$$

is the charge in the metal ($\Delta_{i0} = \phi_m - \chi_s - q\varphi_{b0}$ is the potential drop in the intermediate layer in the absence of bias voltage (Fig. 1), $\varepsilon_i = \varepsilon_0\varepsilon_{ri}$ is the permittivity, ε_{ir} is the relative permittivity, ε_0 is the absolute permittivity of vacuum, and $C_{\delta i} = \varepsilon_i/\delta_i$ is the capacitance of the insulating layer between the metal and semiconductor),

$$Q_{sc}(V) = \left(2\varepsilon_s qN_D(V_D - V_b - kT/q)\right)^{1/2} \tag{11}$$

is the space charge in the barrier, $\varepsilon_s = \varepsilon_0\varepsilon_{sr}$ is the permittivity, ε_{sr} is the relative permittivity of the semiconductor, and $V_D = \varphi_{b0} - \varphi_s$ is the diffusion potential of the barrier.

In the general case, the charge of surface states involves the charge of states, which are in equilibrium (communicate) with the metal (Q_{ssm}) and semiconductor (Q_{sss}),[1]

$$Q_{ss} = Q_{ssm} + Q_{sss}. \tag{12}$$

The role of the first type of states can be performed, for example, by metal induced gap states (MIGS).[1] Their density N_{ssm} is high, and their energy distribution can be assumed to be constant in the first approximation. These states providing the pinning of the Fermi level near a certain level E_{b0} practically define the barrier height at equilibrium ($\varphi_{b0} = E_c - E_{b0}$) (Fig. 1), which depends on the state density and the position of the charge neutrality level of the surface φ_{CNL} counted off from the valence band top.[1,2] (The position of φ_{CNL} in Fig. 1 corresponds to the equilibrium state.) The state charge Q_{ssm} is represented in the following form in the $T = 0$ approximation for the distribution function:

$$Q_{ssm}(V) = -qN_{ssm}(E_g - \varphi_{CNL} - q\varphi_{b0} - qV_{\delta i}). \tag{13}$$

The distribution of ISs communicating with a semiconductor is accepted in the form of two exponents (i.e., close to the U-shaped form[30,31])

$$N_{sssA}(E) = N_{sA}^0\exp\left(\frac{E_c - E}{E_{0A}}\right), \quad N_{sssD}(E) = N_{sD}^0\exp\left(\frac{E - E_v}{E_{0D}}\right), \tag{14}$$

where N_{sA}^0 and N_{sD}^0 are the densities of acceptor and donor states near the conduction band bottom ($E = E_c$) and the valence band top ($E = E_v$), respectively, E_{0A} and E_{0D} are the decay constants of the state densities (negative quantities) independent of energy. A reverse distribution of ISs - donor states in the upper part of the forbidden gap and acceptor states in the lower part of the forbidden band - (replacement of indices $A \to D$ and $D \to A$ in Eq. (14)) gives a qualitatively similar physical result, because a decrease of the positive charge of donor ISs with bias increasing results in the similar effect, as an increase of the negative charge does. However, in the last case, a marked, sometimes a substantial, change in the barrier height at the contact can be observed at high IS densities (see below).

The IS charge can be found by integrating over the whole bandgap. When choosing the distribution function in a piecewise-linear approximation[31,39] (to increase the accuracy), the expressions for the charges can be obtained in analytical form. The ideality factor n of IVC is given by the expression[38]

$$n = 1 + \frac{C_{sc} + C_{sss}}{C_{\delta i} + C_{ssm}}, \tag{15}$$

where C_{sc}, $C_{sss} = C_{ssA} + C_{ssD}$, and C_{ssm} are the capacities of the Schottky barrier, acceptor and donor ISs, and states which are in equilibrium with the metal, respectively, obtained by differentiation of the corresponding charges.

Figure 2 gives an overview of the effect of ISs communicating with the semiconductor on the *I-V*-characteristics of the contact. The values of the model parameters selected for demonstration correspond, as a whole, to well documented data (or close to them) and to the values commonly used in the calculations: N_{ssm}= 10^{14} cm^{-2} eV^{-1}, $\varphi_m - \chi_s$= 0.9 V, ϕ_{CNL}= 0.5 eV, R^*= 8.156 A/cm^{2}K^2, δ_i= 10^{-7} cm, and ε_{ir}= 1. The impurity concentration and contact diameter ($N_D = 1 \times 10^{16}$ cm^{-3}, $D = 5$ μm) approximately correspond to the real values for examined structures. Parameters of the IS distribution are listed in the caption and in the figure.

The *I-V*-characteristics presented in the figure correspond to the different positions of ISs: In Fig. 2(a), acceptor states are in the upper part of the bandgap and the donor states are in the lower part of the bandgap, whereas in Fig. 2(b)*)*, a reverse situation is presented. In both cases, an equality of densities of both states at the level $N^0_{sD} = N^0_{sA}$= 3×10^{12} cm^{-2} eV^{-1} ($E_{0A} = E_{0D} \equiv E_0 = -0.12$ eV) was assumed for the initial state. At these densities and at lower ones, practically no effect of these states is observed. *I-V*-characteristics that are located above (to the left) of the initial characteristic correspond to an increase in the donor state density (it is shown in the inset by triple lines of the IS distribution). *I-V*-characteristics that are located below (to the right) of the initial characteristic correspond to an increase in the density of acceptor states (it is also shown in the inset). As can be seen, in the first case (Fig. 2(a)), the acceptor states can markedly change the ideality factor and the measured barrier height, whereas the effect of donor states is not essential (since most of them are in the neutral state). In the second case (Fig. 2(b)), on the contrary, the donor states can greatly reduce the barrier height and the acceptor states can greatly increase it.

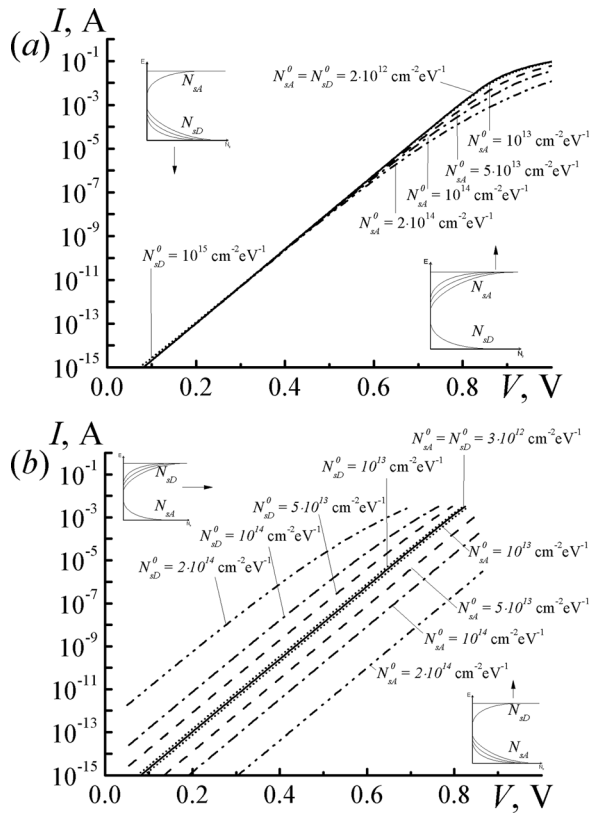

FIG. 2. *I-V*-characteristics of a contact corresponding to the Bardeen model for different location of interface states: (a) – acceptor states in the upper part of the bandgap and donor states in the lower part of the bandgap, (b) – donor states in the upper part of the bandgap and acceptor states in the lower part of the bandgap; N^0_{sA} and N^0_{sD} – the densities of acceptor and donor states near the bandgap edges, $E_{0A} = E_{0\,D} \equiv E_0 = -0.12$ eV.

B. A model of an intimate contact with SSSs

Energy diagram of an intimate M-S contact is demonstrated in Fig. 3 for the case of a continuous spectrum of surface states inhomogeneously distributed over energy and coordinate having taken into account the image-force effect. The pictured model corresponds to the three different situations: (1) the absence of the SSSs communicating with the semiconductor; (2) the presence of only the acceptor SSSs in the lower part of the bandgap; and (3) the presence of only the donor states in the upper part of the bandgap. The model parameters selected for demonstration are shown in the figure caption. Additional parameters (as compared to the Bardeen model) are the decay constants of the SSS densities deep into the semiconductor (see below). Note that in this case, instead of the state density communicating with the metal, the barrier height directly on the M-S interface ($\varphi^0_b = 0.9$ B) is defined without specifying a mechanism for maintaining its constant value.

A characteristic feature of the intimate contact diagram is the change of the barrier height and deformation of its shape (the displacement of the barrier maximum deep into the semiconductor more clearly shown in the inset of the figure). These changes are caused both by the image-force effect and by the presence of SSSs. The reasons for such

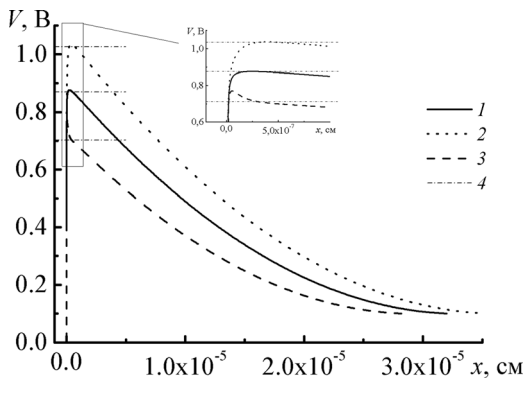

FIG. 3. Energy diagram of an intimate M-S contact for different values of the SSS parameters: 1 – in the absence of SSSs, 2 – in the presence of only acceptor states in the lower part of the bandgap, 3 - in the presence of only donor states in the upper part of the bandgap, 4 – the level corresponding to the maximum tunnel current ($N^0_{sD} = N^0_{sA}$= 10^{14} cm^{-2} eV^{-1}, $E_{0A} = E_{0D} \equiv E_0 = -0.12$ eV, $\lambda_A = \lambda_D \equiv \lambda$ = 10^{-7} cm. Other parameters: φ^0_b= 0.9 V, $N_D = 1 \times 10^{16}$ cm^{-3}).

changes are associated with the requirement of the contact neutrality in the presence and in the absence of SSSs at simultaneous conservation of the barrier height $\varphi_b^0 = 0.9$ V directly at the M-S interface.[32] The appearance of a negative charge on the acceptor SSSs leads to an increase in the positive barrier space charge (for its compensation) and, as a result, to an increase in the barrier height (curve 2). The appearance of a positive charge on the donor SSSs results in a decrease in the barrier space charge and a significant thinning of the barrier in the region of the SSS localization. Due to the tunnel effect, this leads to a decrease in the effective barrier height (curve 3 and level 4 in Fig. 3).

As a result of changes in the height and shape of the barrier, a series of anomalies in the behavior of the *I-V*-characteristics, including "low-temperature anomaly," appears.[32] The shape of the potential barrier is determined by the two components associated with the space and SSSs charges ($V_P(x)$) and with the image-force effect ($V'(x)$),

$$V(x) = V_P(x) + V'(x) = V_P(x) - \frac{q}{16\pi\varepsilon_s(W-x)}. \quad (16)$$

The first component $V_P(x)$ is defined from the solution of the Poisson's equation, which includes the charges of acceptor $\rho_A(x)$ and donor $\rho_D(x)$ subsurface states along with the impurity and electron charges. Energy distribution of these states is fully consistent with Eq. (14). Their distribution over the coordinate with the decay constants λ_A and λ_D is also taken into account. Volume charge densities of these states are represented as follows:[32]

$$\rho_A(x) = -\frac{qN_{sA}^0}{\lambda_A}\exp\left(-\frac{W-x}{\lambda_A}\right) \times \int_{E_V(x)}^{E_c(x)} f_A(E,E_F)\exp\left(\frac{E_c(x)-E}{E_{0A}}\right)dE, \quad (17)$$

$$\rho_D(x) = \frac{qN_{sD}^0}{\lambda_D}\exp\left(-\frac{W-x}{\lambda_D}\right) \times \int_{E_V(x)}^{E_c(x)} (1-f_D(E,E_F))\exp\left(\frac{E-E_v(x)}{E_{0D}}\right) dE. \quad (18)$$

To simplify the calculations, a piecewise linear approximation for the distribution functions was used. As a result, the expressions for $\rho_A(x)$ and $\rho_D(x)$ can be obtained in analytical form. We also consider the opposite position of SSSs: Donor states near the conduction band and acceptor states - near the valence band.

The boundary condition at $x = W$ (M-S interface) with allowance for the applied bias V_b takes a form,

$$V(W) = \varphi_b^0 - \varphi_s - V_b \quad (19)$$

(here, to eliminate confusion between the potential and bias voltage at the contact, the latter is designated as V_b). Note that for ease of demonstration of the barrier shape, a M-S interface is taken as the reference point ($x = 0$) in Fig. 3.

Distortion of the barrier shape, as already mentioned, increases the role of tunneling in the current flow. In the presence of donor states, the maximum of tunneling current markedly sinks below the top of the barrier, even at a selected impurity concentration of 1×10^{16} cm^{-3}: line 4 in Fig. 3. For this reason, the current through the contact is determined with allowance for the tunneling component in the form,[41]

$$I = \frac{AR^{\bullet}T}{k}\exp\left(-\frac{q\varphi_s}{kT}\right)\int_0^{\infty} T_t(E)\exp\left(-\frac{E}{kT}\right)dE \times \left[1-\exp\left(-\frac{qV_b - IR_s}{kT}\right)\right]. \quad (20)$$

Here T_t is the transparency of the barrier in the WKB-approximation,

$$T_t(E) = \exp\frac{-4\pi}{h}\int_{x_1}^{W}\left\{2m^*[qV(x)-E]\right\}^{1/2}dx, \quad (21)$$

h is the Planck constant, and m^* is the electron effective mass.

Typical *I-V*-dependencies calculated in accordance with Eq. (20) using practically the same set of parameters that were used in the Bardeen model, demonstrate a complete qualitative similarity of influence of the donor and acceptor states in both cases (in so doing, we assumed that $\lambda_A = \lambda_D = \lambda = 10^{-7}$ cm). For this reason, we present here no *I-V*-characteristics. As shown by previous studies,[32] the influence of λ is qualitatively similar to that of the state density at the interface, i.e., the effect increases with increasing λ. The observed close similarity in the behavior of the two models is essentially the main result of the comparison. However, the mechanism of the effect of SSSs on the behavior of IVC is quite different from that of IS effect mechanism. In the Bardeen model, changes in the barrier height and, consequently, changes in IVCs are due to the potential drop in the intermediate layer $V_{\delta i}$, which depends on the nature and distribution of ISs. In the IC model, the change in the height and shape of the barrier (and, consequently, the change in IVC) is due to the penetration of SSSs in the barrier region and conservation of the barrier height at the M-S interface under applied bias voltage (see above).

III. RESULTS OF EXPERIMENT

Main experimental studies are carried out on the contacts Au-n-GaAs (100) formed on the wafers of ingot material with an impurity concentration of 2.4×10^{16} cm^{-3}. The surface of the wafers has been prepared using standard procedure with chemical-dynamic polishing and wet etching. Contacts with the diameters 5 − 500 μm were formed in the windows in a 0.3 μm thick silicon oxide deposited by pyrolytic oxidation of monosilane at 360 °C. The 0.2 μm thick golden layers were deposited by electrochemical deposition from an electrolyte based on potassium dicyano aurate (I). Pretreatment of the surface in the windows just before the deposition of metal included the degreasing, removal of own oxide in a sulfuric acid etchant H_2SO_4: H_2O = 1: 10, and

washing in de-ionized water, after which the samples were immersed in a bath for the deposition.

Typical experimental *I-V*-dependencies for the contacts Au-n-GaAs with the diameters 500, 50, and 5 μm are shown in Fig. 4. These dependencies can be fitted with high accuracy by theoretical dependencies obtained on the base of the Bardeen and IC models using the same sets of ISs and SSSs, respectively, for all diameters. The fitting curves are indistinguishable in the figure. The procedure of fitting the theoretical curves to the experimental ones (in the Bardeen model) starts from the measured values of the barrier height and ideality factor, from "reasonable" values of the state density communicating with the metal N_{ssm}, and parameters of the intermediate layer δ_i and ε_i. Then, using Eqs. (1), (3), and (9)–(15), a stepwise construction of the dependence $\varphi_b(V) \equiv \varphi_{bI}$ was performed (see Eqs. (2) and (7)) to describe the experimental *I-V*-characteristic with maximum accuracy in the widest range of bias (currents). In addition, the fitting values of R_s were taken into account. Of course, we cannot exclude the situations, where more than one set of contact parameters is acceptable. We consider that the main criterion for selection of the parameter set is its simultaneous acceptability to the *I-V*-characteristics for different contact diameters and to all the experimental dependences of the barrier heights and ideality factor on the bias voltage and contact diameter (see below).

For intimate contact, the barrier shape is calculated from the Poisson equation[32] taking into account Eqs. (16)–(19) (in zeroth approximation, the value φ_b^0 was defined from the experimental IVC in accordance with Eq. (6)). On the basis of the calculated barrier shape, an *I-V*-characteristic was constructed according to Eqs. (20) and (21), from which the ideality factor and the measured and effective barrier heights were determined with the help of Eqs. (4)–(7). Then, further fitting was performed after comparing these parameters with experimental values. The final parameters of the models are listed in the caption of Fig. 4. The fitting ideality factors of IVCs (at a current of 10^{-6} A) correspond to the experimental values. As expected, they increase with decreasing diameter and are 1.033, 1.046, and 1.07, respectively. The calculated barrier height in the Bardeen model is $\varphi_{b0} = 0.859$ V. Naturally, in the IC model, an effective barrier height taking into account the image-force and tunneling effects is also equal to this value, since the calculated characteristics for both models nicely fit the experimental IVCs.

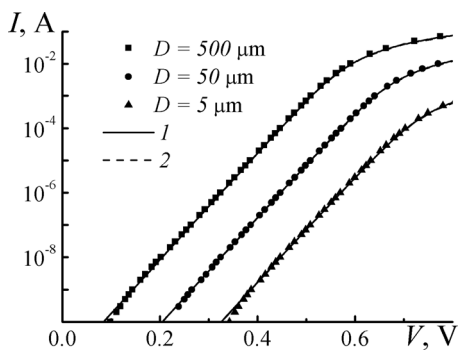

FIG. 4. Experimental (points) and calculated (1 – for Bardeen model, 2 – for IC model) *I-V*-characteristics of the contacts Au-n-GaAs with the diameters of 500, 50, and 5 μm; specified parameters of the Bardeen model: $\phi_m - \chi_s = 1.03$ V, $\phi_{CNL} = 0.562$ eV, $N_{ssm} = 10^{14}$ cm^{-2} eV^{-1}, $\delta_i = 10^{-7}$ cm, $\varepsilon_{ir} = 1$; fitting parameters of the Bardee model: $N_{sD}^0 = N_{sA}^0 = 1.9 \times 10^{13}$ cm^{-2} eV^{-1}, $E_0 = -0.25$ eV; fitting parameters of the IC model: $\varphi_b^0 = 0.902$ B, $N_{sD}^0 = N_{sA}^0 = 1.2 \times 10^{13}$ cm^{-2} eV^{-1}; $\lambda = 8 \times 10^{-8}$ cm, $E_0 = -0.17$ eV ($R^* = 8.156$ A/cm^2 K^2, $N_D = 2.4 \times 10^{16}$ cm^{-3}).

Figures 5(a) and 5(b) show the experimental bias dependencies of the ideality factor of IVC, the measured (φ_{bm}) and effective (φ_{bI}) barrier heights determined by Eqs. (5)–(7), as well as the magnitude $\varphi_{bn} = n\varphi_{bm}$ for contacts, whose IVCs are presented in Fig. 4. It should be clarified that actually, the values of n related to a given bias, were measured in the range of the current variation within one order of magnitude (the same applies to the measurements at a given current in Fig. 6). For this reason, the theoretical values of n (and φ_{bm}) were calculated in the same way for the correct comparison with experiment. The systematic error of this approach of the determining n is less than 0.02 and does not affect the principal regularities.

As can be seen, all the experimental dependencies in Fig. 5 are quite well approximated by the calculated curves for both considered models of the contact at the same values of the IS and SSS distribution parameters, which are calculated by fitting to the experimental IVCs in Fig. 4. Their nonlinear character is in full compliance with the nonlinear (exponential) increase in the state density to the bottom of the conduction band assumed in explanation of IVC. Figure 5(a) also shows the contribution from the tunnel current to

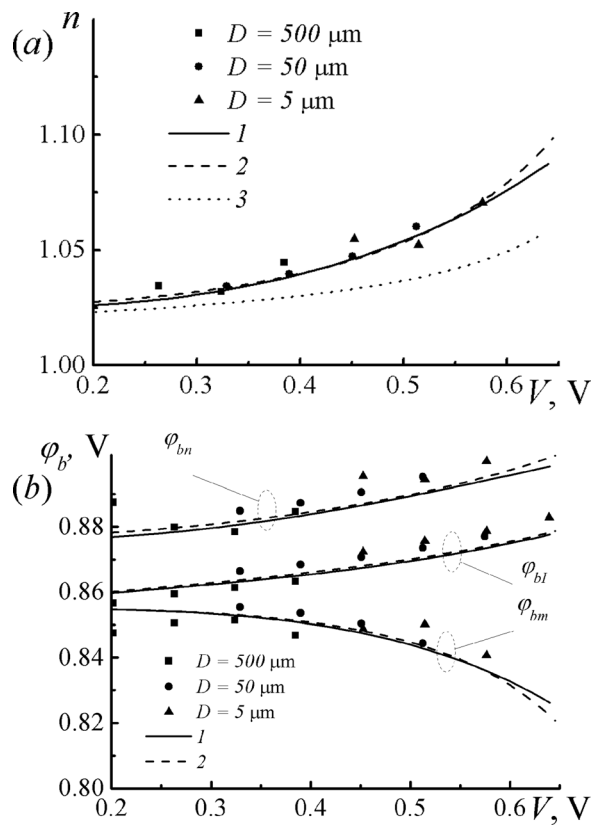

FIG. 5. Bias dependencies of the ideality factor – (a) and the effective (φ_{bI}) and measured (φ_{bm}) barrier heights and the quantity $\varphi_{bn} = n\varphi_{bm}$- (b): the points show the experimental data for contacts with the diameters 500, 50, and 5 μm, 1 – Bardeen model, 2 – IC model, 3 (in a) – contribution from the tunneling effect; parameters of the models are the same as in Fig. 4.

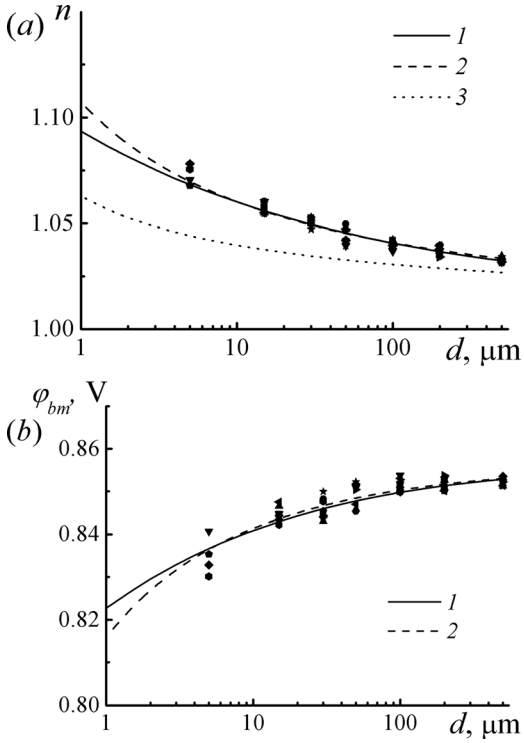

FIG. 6. Dependencies of the ideality factor n – (a) and measured barrier height φ_{bm}- (b) on the contact diameter: the points show the experimental data, 1 – Bardeen model, 2 – IC model, dashed lines (in a) – contribution from the tunneling effect; parameters of the models are the same as in Figs. 4 and 5.

the dependence $n(V)$. It should be especially noted (Fig. 5(b)) that with increasing bias voltage (and hence, with increasing ideality factor (Fig. 5(a))), the measured barrier height φ_{bm} defined by Eq. (6) decreases. But the effective barrier height φ_{bI} increases according to Eq. (7). It is important to emphasize this fact, because the confusion of these terms reflects confusion in the interpretation of the physical relation between the ideality factor and barrier height.

Figures 6(a) and 6(b) demonstrate typical dependences of the ideality factor n and measured barrier height φ_{bm} on the contact size (diameter). Recall that these parameters were measured at the same current (more precisely, in the same range of currents 10^{-6} – 10^{-5} A), regardless of the diameter of the contact. For both dependencies, $n(d)$ and $\varphi_{bm}(d)$, good agreement with the calculation is observed for the same parameters of models that were obtained for the IVCs in Fig. 4. Thus, the nature of the dependencies $n(d)$ and $\varphi_{bm}(d)$ (the presence of edge effects in the contact) can be nicely explained within the concept of the effect of the nonlinear bias dependence of the barrier height on the "abnormal" behavior of the measured parameters of the SB contact. In our case, the specific reason for the edge effects is the inhomogeneous distribution of ISs and SSSs over energy and coordinate. The dashed line in Fig. 6(a) illustrates the contribution from the tunneling component to the dependence $n(d)$ for an intimate contact.

Of particular interest are the experimental dependencies $\varphi_{bm}(n)$ in Figs. 7 and 8. The first dependence is based on the data presented in Figs. 6(a) and 6(b), the second one is constructed on the basis of results obtained for a specially

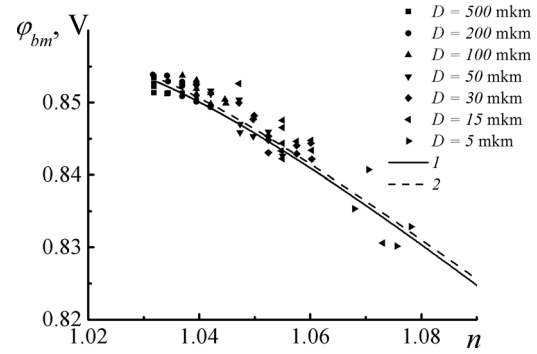

FIG. 7. Relation between the measured barrier height φ_{bm} and ideality factor n for contacts with different diameters: the points show the experimental data, 1 – Bardeen model, 2 – IC model; parameters of the models are the same as in Figs. 4–6.

selected contact with the diameter of 5 μm and a broader set of values of the ideality factor. These dependencies correspond generally to the well-known dependencies for a wide range of contacts (see, for example, Refs. 8–11). Almost always, they are explained by an inhomogeneous distribution of the barrier height over the contact area in the version of the model of "saddle points."[14,15] However, we can at least say that the explanation of the dependence $\varphi_{bm}(n)$ has a broader theoretical framework. In particular, it can be explained on the basis of considered models of contact with an inhomogeneous density distribution of ISs and SSSs over energy and coordinate and lateral inhomogeneity of the parameter distribution. This is supported by a favorable agreement between theory and experiment.

The theoretical (fitting) dependencies in Fig. 7 are based on the same parameters of models that have been used before. However, in the case of Fig. 8, the experimental dependencies are explained by the lateral variations of the contact parameters, but not by the fact that these parameters are measured at a specified current and different biases (as in Fig. 7). As is demonstrated by fitting the parameters of ISs

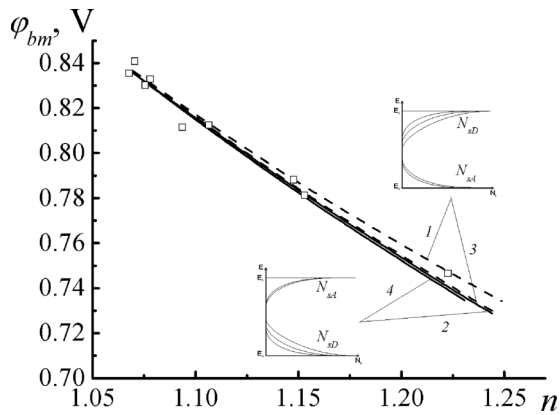

FIG. 8. Relation between the measured barrier height φ_{bm} and ideality factor n for contacts with the diameter of 5 μm: the points show the experimental data, solid lines – Bardeen model, dashed lines – IC model; lines 1 and 3 – fitting is made due to the increase in the density of donor states (up to 1×10^{14} and 6.9×10^{13} cm^{-2} eV^{-1}, respectively) and partly acceptor states (up to 7.07×10^{13} and 3.9×10^{13} cm^{-2} eV^{-1}, respectively); lines 2 and 4 – fitting is made due to an increase in the density of donor states (up to 3.72×10^{14} and 2.19×10^{14} cm^{-2} eV^{-1}, respectively) and the constant E_0 (up to −0.35 and −0.45 eV, respectively).

and SSSs to the experimental dependence $\varphi_{bm}(n)$, for both considered models, the best result can be achieved mainly by increasing the density of donor states regardless of their location in the upper (lines 1(IC model) and 3(BM)) or lower (lines 2 (IC model) and 4 (BM)) part of the bandgap. In addition, for the cases of fitting lines 1 and 3, an additional increase in the density of acceptor states is needed at fixed values of parameters of the IS and SSS distributions (E_0). Changes in the ISs and SSSs are shown in the insets in Fig. 8. The values of state densities previously obtained from fitting to Figs. 4–7 are taken as initial values.

For the cases corresponding to fitting lines 2 and 4, the density of acceptor states remains unchanged. However, for effective fitting, the distribution parameter of the state density should be increased, which, in our opinion, makes the first version of fitting (see above) more preferable. It should be made clear that the procedure used for the parameter fitting is based on the assumption that the different IS and SSS parameters characterize the different contacts, whereas, the parameters of each individual contact are constant.

IV. DISCUSSION

The more than satisfactory agreement between the calculated and experimental dependencies, and the reality of basic assumptions, suggest the validity of the proposed physical models for the interpretation of the SBC characteristics. In principle, this behavior of contacts, including their "low-temperature anomaly" of IVCs, can be explained by any reasonable physical model, which leads to a nonlinear bias dependence of the barrier height[26,28,30–32,33–36] (see Introduction). We can also assume that the observed "anomalous" dependencies can be explained by a nonuniform distribution of the barrier height in the contact within the model of "saddle points"[14,15,25] (see Introduction). Indeed, it allows us to satisfactorily describe the experimental dependencies by choosing the distribution parameters.[9,22] But the existing interpretation of experimental data on the basis of the theoretical model of "saddle points" raises a number of problems. According to Refs. 9 and 15, to simplify the analytical estimates, it is assumed that the M-S contact consists of a homogeneous part with the constant barrier height and areas with low barrier heights (LBH) in the form of "saddle points." These latter are characterized by a Gaussian distribution of the combined parameter of "saddle points" $\gamma = 3(\Delta R_0^2/4)^{1/3}$, where Δ is a decrease in the barrier height at the M-S interface just above the "saddle point" (the metal is on top) and R_0 is the radius of the patch with lower barrier height. Total current in such a contact, including thermo-emission current in the uniform part and region with "saddle points" (averaged diode), is represented in the following form (for simplicity, series resistances are omitted):

$$I = AR^*T^2\exp\left(-\frac{q\varphi_b^0}{kT}\right)\left[\exp\left(\frac{qV}{kT}\right)-1\right][(1-\bar{A}_{eff\,p}) + \bar{A}_{eff}\exp(\beta\Delta\bar{\varphi}_{bef})], \quad (22)$$

where

$$\bar{A}_{ef} = \frac{4\pi c\sigma_\gamma^2\eta^{1/3}}{9V_D^{1/3}} \quad (23)$$

is the effective area relative to the contact area,

$$\bar{\varphi}_{bef} = \varphi_b^0 - \Delta\bar{\varphi}_{bef} = \varphi_b^0 - \frac{\beta\sigma_\gamma^2 V_D^{2/3}}{2\eta^{2/3}} \quad (24)$$

is the effective barrier height in the region with "saddle points," $\Delta\bar{\varphi}_{bef}$ is the effective decrease of the barrier height in this region, c is the density of "saddle points" in the contact, $\sigma\gamma$ is the standard deviation in the distribution of the parameter γ, $V_D = \varphi_b^0 - \varphi_s - V_b$, and $\beta = q/kT$. It is this characteristic that is then compared with the experimental one.

First of all, it should be said that the use of the Gaussian distribution of the "saddle points" (and other inhomogeneities) in the contacts with edge effects seems to be incorrect. The presence of these effects should be controlled not only at room temperature, but also at low temperatures, where they manifest themselves much more markedly.[5,6] There are also other problems with Eq. (22), as can be seen from the following.

A major shortcoming of Eq. (22) is that the regions with the conventional lowering of the barrier height (LBH) (i.e., without "saddle points") are ignored. The appearance of these areas in some situations may be more likely than the appearance of a "saddle point." Obviously, for example, that at the periphery of the contact, the condition of total surrounding of the region with the LBH by the area with the much greater barrier height seems unlikely. That is, more likely is the appearance of conventional regions with LBH. Therefore, these large regions that do not satisfy the above condition, and hence have an obviously lower barrier height than that in the "saddle points," must determine the low-temperature and other distortions of the IVCs.

Highly questionable is the way the effect of the series resistance of the regions with "saddle points" is taken into account. In some works (Ref. 9 and others), this effect is taken into account by replacing V_b for $V_b - IR_s$, where R_s is the integral series resistance of the whole contact. The author of the model[25] pointed out how this approach is incorrect. A significant influence of the series resistance of "saddle points" may be due to their small area ($\bar{A}_{ef} \ll 1$). Note also that for the case of common Gaussian distribution of the barrier height, the series resistance of regions with LBH results in a "low-temperature anomaly" of IVC.[33,34]

Finally, one more important circumstance is pointed out by the author of the model.[15] This is the need to take into consideration the bias dependence of the ideality factor, or in other words, the nonlinear bias dependence of the effective barrier height. Effective barrier height for the forward IVC, Eq. (22), which we denote simply $\varphi_b(V)$ (as defined in Eq. (2)), can be obtained from comparing the I-V-characteristics in the forms (22) and (2). As a result, we obtain the following expression (at $\bar{A}_{ef} \ll 1$):

$$\varphi_b(V) = \varphi_b^0 - \frac{kT}{q}\ln[1 + \bar{A}_{ef}\exp(\beta\Delta\bar{\varphi}_{bef})]. \quad (25)$$

If the "saddle points" play the dominant role in the current flow through the contact ($\bar{A}_{ef}\exp(\beta\Delta\bar{\varphi}_{bef}) \gg 1$), expression[25] is transformed to the form

$$\varphi_b(V) \cong \varphi_b^0 - \Delta\bar{\varphi}_{bef} - \frac{kT}{q}\ln\bar{A}_{ef}. \quad (25a)$$

For a given current (when $\varphi_b(V) \equiv \varphi_{bI}$), which is natural for measurements in the temperature range, or for contacts with different diameters, the relationship between the effective and measured barrier height of the contact is determined by a simple relation (7),

$$\varphi_{bn} = n\varphi_{bm} = \varphi_b^0 - \Delta\bar{\varphi}_{bef} - \frac{kT}{q}\ln\bar{A}_{ef} + (n-1)\frac{kT}{q}\ln\frac{AR^*T^2}{I}. \quad (26)$$

Obviously, to represent the IVC of an inhomogeneous contact with "saddle points," we can use the *I-V*-characteristic, which was used before for all contacts with the nonlinear bias dependence of the barrier height,[28,31,32,34–36]

$$I = AR^*T^2\exp\left(-\frac{q\varphi_{bn}}{nkT}\right)\exp\left(\frac{qV}{nkT}\right) = I_s\exp\left(\frac{qV}{nkT}\right), \quad (27)$$

where the barrier height $\varphi_{bn} = n\varphi_{bm}$ (and hence, the measured barrier height φ_{bm}) is uniquely related to the effective barrier height $\varphi_b(V)$ according to Eq. (26). We believe that it is important to emphasize the difference between these values because they are often identified in known experimental works.

V. CONCLUSION

This paper presents the results of studying the *I-V*-characteristics of the contacts Au-n-GaAs obtained by electrochemical deposition. The observed special features of the characteristics (the bias dependencies of the ideality factor and the measured and effective barrier heights, the inverse relationship between the measured barrier height and ideality factor, and edge effects, that is, the dependence of the parameters on the diameter) are explained by the nonlinear bias dependence of the effective barrier height on the basis of the model of a contact with an intermediate layer and interface states (Bardeen model) and the model of an intimate contact with subsurface states. The nonlinearity of the bias dependence of the barrier height is due to the non-uniform energy distribution of interface states (a decrease of state density from the edges to the middle of the bandgap) and inhomogeneous, not only over energy, but also over coordinate (from the surface to the depth), distribution of subsurface states. For all contact diameters, the main features of the *I-V*-characteristics are explained using the one set of parameters own for each of the models.

It is also essential condition for each of the models that the barrier height and ideality factor are measured at the same (specified) current when measuring the contacts with different diameters (and during the temperature measurements - at different temperatures). This condition is not difficult to achieve, but it gives the necessary certainty to the values of barrier heights used in the experiment.

ACKNOWLEDGMENTS

The authors would like to express their thanks to the technological department of CJSC "Scientific Research Institute of Semiconductor Devices" and especially to V. N. Romanovskaya for preparation of samples.

[1]E. H. Rhoderick and R. H. Williams, *Metal-Semiconductor Contacts*, 2nd ed. (Clarendon Press, Oxford, 1988).
[2]E. L. Wall, Solid-State Electron. **19**, 389 (1976).
[3]V. G. Bozhkov and O. Yu. Malakhovsky, Izv. Vuzov. Fiz. **26**, 101 (1983).
[4]V. G. Bozhkov and O. Yu. Malakhovsky, Elektron. Tekh. Ser. 2 **5**, 9 (1987).
[5]M. Wittmer, Phys. Rev. B **42**, 5249 (1990).
[6]M. Wittmer, Phys. Rev. B **43**, 4385 (1991).
[7]M. A. Yeaganeh, Sh. Rahmatollahpur, R. Sadighi-Bonabi, and R. Mamedov, Physica B **405**, 3253 (2010).
[8]A. Martinez, D. Esteve, J. M. Peyriquier, J. M. Lagorse, and D. Dameme, in *Proceedings Manchester Conference Metal-Semiconductor Contacts*, Institute of Physics, London, Conference Series No. 22 (Institute of Physics, London, 1974), p. 67.
[9]R. F. Schmitsdorf, T. U. Kampen, and W. Monch, J. Vac. Sci. Technol. B **15**, 1221 (1997).
[10]W. Mönch, J. Vac. Sci. Technol. B **17**, 1867 (1999).
[11]H. Korkut, N. Yidirim, and A. Turut, Microelectron. Eng. **86**, 111 (2009).
[12]W. Mönch, "Electronic properties of semiconductor interfaces " *in Springerand Photonic Materials,* edited by S. Kasap and P. Caper (Springer, Berlin, 2006), pp. 147–160.
[13]J. H. Werner and H. H. Guttler, J. Appl. Phys. **69**, 1522 (1991).
[14]J. P. Sullivan, R. T. Tung, M. R. Pinto, and W. R. Graham, J. Appl. Phys. **70**, 7403 (1991).
[15]R. T. Tung, Phys. Rev. B **45**, 13509 (1992).
[16]W. J. Kaiser and L. D. Bell, Phys. Rev. Lett. **60**, 1406 (1988).
[17]H. Palm, M. Arbes, and M. Schulz, Phys. Rev. Lett. **71**, 2224 (1993).
[18]A. A. Talin, S. R. Williams, B. A. Morgan, K. M. Ring, and K. L. Kavanagh, Phys. Rev. B **49**, 16474 (1994).
[19]H. Sirringhaus, T. Meyer, E. Y. Lee, and H. van Kanel, Phys. Rev. B **53**, 15944 (1996).
[20]C. Detavernier, R. L. Van Meirhaeghe, R. Donaton, K. Maex, and F. Cardon, J. Appl. Phys. **84**, 3226 (1998).
[21]G. M. Vanalme, G. M. L. Goubert, R. L. Van Meirhaeghe, F. Cardon, and P. Van Daele, Semicond. Sci. Technol. **14**, 871 (1999).
[22]H. -J. Im, I. Ding, J. P. Petz, and W. J. Choyke, Phys. Rev. B **64**, 075310-1 (2001).
[23]S. Forment, M. Biber, R. L. Van Meirhaeghe, W. P. Leroy, and A. Türüt, Semicond. Sci. Technol. **19**, 1391 (2004).
[24]W. R. Leroy, K. Opsomer, S. Forment, and R. L. Van Meirhaeghe, Solid-State Electron. **49**, 878 (2005).
[25]R. T. Tung, Mater. Sci. Eng. R. **35**, 1 (2001).
[26]V. G. Bozhkov, Radiophys. Quantum Electron. **45**, 381 (2002).
[27]V. G. Bozhkov and D. Ju. Kuzyakov, J. Appl. Phys. **92**, 4502 (2002).
[28]V. G. Bozhkov and S. E. Zaitzev, Russ. Phys. J. **48**, 312 (2005).
[29]V. G. Bozhkov and O. Yu. Malakhovsky, Izv. Fiz. **26**, 94 (1983).
[30]V. G. Bozhkov, Izv. Vuzov. Fiz. **30**, 29 (1987).
[31]V. G. Bozhkov and S. E. Zaitzev, Radiophys. Quantum Electron. **47**, 688 (2004).
[32]V. G. Bozhkov and S. E. Zaitzev, Russ. Phys. J. **48**, 1085 (2005).
[33]E. Dobrocka and J. Osvald, Appl. Phys. Lett. **65**, 575 (1994).
[34]V. G. Bozhkov and S. E. Zaitzev, J. Commun. Technol. Electron. **52**, 97 (2007).
[35]V. G. Bozhkov and S. E. Zaitzev, Russ. Phys. J. **49**, 251 (2006).
[36]V. G. Bozhkov and A. V. Shmargunov, J. Appl. Phys. **109**, 113718 (2011).
[37]S. M. Sze, *Physics of Semiconductor Devices*, 2nd ed. (Wiley, New York, 1981).

[38]V. G. Bozhkov, N. A. Torkhov, and A. V. Shmargunov, J. Appl. Phys. **109**, 073714 (2011).
[39]V. G. Bozhkov, G. F. Kovtunenko, G. M. Surotkina, and L. S. Selina, Elektron. Tekh. Ser. 2. **4**, 14 (1978).
[40]R. Hackam and P. Harrop, IEEE Trans. **ED-19**, 1231 (1972).
[41]C. R. Crowell and V. L. Rideout, Solid-State Electron. **12**, 89 (1969).
[42]L. F. Wagner, R. W. Joung, and A. Sugerman, IEEE Electron Device Lett. **EDL-4**, 320 (1983).